

# Ambiguity in Resolving the Elastic Parameters of Gas Sands from Wide-Angle AVO

Andrew J. Calvert - Simon Fraser University and David F. Aldridge - Sandia National Laboratories

CSEG Geophysics 2002

## Summary

We investigate the range of elastic parameters that will reproduce the amplitude of P waves reflected at angles of incidence up to  $52^\circ$  from the top-sand and base-sand interfaces of Ostrander's gas sand model. In the case of the top-sand reflector, which lies at the top of a P wave low velocity layer, it is not possible to resolve either density or S wave speed information given P-to-P amplitude data alone. The density contrast is, however, well resolved for the base-sand reflector, but the S wave information remains ambiguous. Including converted P-to-S reflections in the analysis significantly reduces the range of elastic parameters that can reproduce the reflection amplitudes predicted by Ostrander's model. We suggest that differences in the ability to resolve density are related to the existence and location of the P wave critical point, which permits the determination of the P wave speed contrast across an interface.

## 1. Introduction

Following the early work of Ostrander (1984), who demonstrated that P wave reflections from gas sands could exhibit an anomalous amplitude variation with increasing source-receiver offset (AVO), i.e. angle of incidence, considerable effort has been devoted to the extraction of subsurface elastic parameters from the amplitudes of reflected seismic waves. The majority of this work has focussed on the use of P-to-P (P-P) reflections because this wave type is most commonly utilised in conventional exploration surveys. For two homogeneous isotropic elastic media in welded contact, the amplitude of the P-P reflection can be determined at any angle of incidence from the Zoeppritz equations if the six parameters that completely characterise the elastic properties of the two media, for example the densities and wave speeds, are known. A number of linearised approximations to the expression for P wave reflection amplitude, which offer some insight into the factors that control its variation with changing angle of incidence, have been developed (e.g. Aki and Richards, 1980; Shuey, 1985; Smith and Gidlow, 1987; Fatti et al., 1994). These approximations typically break down at angles of incidence greater than 30 degrees, and are only valid for small changes in the elastic parameters across the interface. Nevertheless, the relatively simple form of these expression has facilitated the estimation of parameters, such as P and S reflectivity, from seismic field data in a computationally efficient fashion using least squares methods. The influence of the density contrast across an interface on the P wave reflection amplitude only becomes marked at large angles of incidence, making it difficult to extract density information with approximations that are restricted to small angles. The extraction of density information and the desire to constrain better the S wave speeds has motivated recent interest in the AVO inversion of wide-angle data (Roberts, 2000).

In this paper, we investigate the range of elastic parameters that will reproduce the amplitude of P waves reflected at wide-angle from the top-sand and base-sand interfaces of Ostrander's Class III gas sand model (Ostrander, 1984). We disregard multiples and converted waves that would, in reality, be generated by an embedded layer. For this study, we consider the two interfaces separately and for each interface calculate the amplitude of the P wave reflection over a wide range of angles of incidence using the exact Zoeppritz equations. We then calculate P wave reflection amplitudes for a broad range of material parameters, and determine a root mean square (RMS) misfit function that we use to characterise those parameters that will reproduce the variation of reflection amplitude with angle of incidence for both interfaces of the gas sand model. In an analysis based on a linearised solution to the Zoeppritz equations, Lines (1999) showed that density is poorly resolved by P wave reflection amplitudes recorded over a limited range of angles of incidence from the top of a low impedance contrast gas sand. Our approach allows us to determine the range of elastic parameters that can be resolved at wide angle when the exact Zoeppritz equations are employed. This range of material parameters can be substantially reduced by incorporating additional information from P-to-S (P-S) converted reflections, but we infer that a full 4-parameter AVO inversion may only be possible when the P wave critical angle occurs close to the range of angles over which amplitudes are available.

Shale	$V_p = 3048 \text{ m s}^{-1}$
	$V_s = 1244 \text{ m s}^{-1}$
	$\rho = 2400 \text{ kg m}^{-3}$
<hr/>	
Gas Sand	$V_p = 2438 \text{ m s}^{-1}$
	$V_s = 1626 \text{ m s}^{-1}$
	$\rho = 2140 \text{ kg m}^{-3}$
<hr/>	
Shale	$V_p = 3048 \text{ m s}^{-1}$
	$V_s = 1244 \text{ m s}^{-1}$
	$\rho = 2400 \text{ kg m}^{-3}$

Figure 1. P wave speed,  $V_p$ , S wave speed,  $V_s$ , and density,  $\rho$ , for the different layers of Ostrander's gas sand model shown in SI units.

## 2. Methodology

For both interfaces of the Ostrander model, synthetic P-to-P reflection amplitude data were calculated using the exact Zoeppritz equations as a function of angle of incidence every  $2^\circ$  from  $0^\circ$  to  $52^\circ$ , which is just less than the P wave critical angle of the lower interface. No noise was added to these amplitude data. The values of these synthetic amplitude data thus indicate the reflection coefficient at a given angle of incidence. Using the parameterisation of the Zoeppritz equations discussed below, amplitude values were calculated for a wide range of trial parameter values, and a least-squares-based objective, i.e. misfit, function was calculated. The objective function is the logarithm to the base 10 of the root mean square average of the differences between the synthetic and trial amplitude data; thus, for example, a RMS misfit of 0.01 corresponds to a value of the objective function of  $-2$ . This formulation of the objective function was chosen primarily to facilitate display of the function's values. Low amplitude values of the objective function indicate the ranges of material parameters in model space that are able to reproduce well the original synthetic amplitude data. We have arbitrarily chosen a value of the objective function of  $-2$ , i.e. a RMS misfit of 0.01, as the cutoff point that indicates the amplitude data have been well fit. A misfit as low as this would only be possible in high quality field data but is not completely unrealistic.

### 2.1 Parameterisation of the Zoeppritz Equations

P wave reflection amplitudes can be computed from the P and S wave speeds plus the densities of the two media in contact, i.e. six parameters. However, the material properties can be specified in the Zoeppritz equations in terms of only four independent variables, which describe the ratios of various elastic properties (Koefoed, 1962), for example  $V_{P2}/V_{P1}$ ,  $V_{S1}/V_{P1}$ ,  $V_{S2}/V_{P1}$ , and  $\rho_2/\rho_1$ , where  $V_P$ ,  $V_S$  and  $\rho$  refer to the P wave speed, S wave speed, and mass density of the two media, and 1 and 2 refer to the upper and lower layers respectively. Consequently doubling the densities and wave speeds of two layers in contact does not change the amplitude of the reflected, or indeed transmitted, waves. As a result, any approach to invert the reflection amplitudes can only recover these four ratios, or some function thereof, rather than individual parameters such as density or S wave speed, and any background wave speed cannot be resolved from amplitude data alone.

The above parameter ratios can be rearranged to provide several other 4-element parameter sets. For our study we have chosen to calculate the objective function as a function of (i) the normal incidence P wave reflection coefficient,  $R_p$ ; (ii) the  $V_s/V_p$  ratio in the upper layer; (iii) the  $V_s/V_p$  ratio in the lower layer; (iv) a density ratio,  $\rho_2/\rho_1$ , which is the ratio of the density of the lower layer to the density of the upper layer. As will be seen later this parameter choice has the merit in some situations of restricting ambiguity in material properties to the hyper-plane in model space defined by the two  $V_s/V_p$  ratios. Furthermore, what is strictly speaking a four-parameter problem can be reduced to three parameters by assuming that the value of  $R_p$  is known. This is a reasonable assumption since, the zero-offset reflection coefficient is the parameter that is best constrained by linearised AVO inversion methods. We are, of course, assuming that the seismic data have been well calibrated to indicate reflection coefficient. Data calibration is not an issue that we address here, but we note that this can, for example, be accomplished in deep-water marine data using the seafloor multiple sequence.

### 2.2 Restrictions on the Values of Elastic Parameters

In order to sample the model space as completely as possible, it is necessary to determine the range of parameter values that are consistent with the theory of linear elasticity. In the absence of a vacuum, mass density is always positive. The strain energy of a linear elastic solid is also positive. For an isotropic solid, positive strain energy implies that the shear modulus,  $\mu$ , and the bulk modulus,  $\kappa$ , which is also known as the incompressibility, are positive (e.g. Debski and Tarantola, 1995). Since the incompressibility is a function of the first Lamé parameter,  $\lambda$ :

$$\kappa = \lambda + \frac{2}{3}\mu \quad , \text{ we must have} \quad \lambda > -\frac{2}{3}\mu .$$

The Lamé parameter,  $\lambda$  can thus be negative, and these negative values correspond to materials with negative Poisson's ratios such as  $\alpha$ -cristobalite (Yeganeh-Haeri et al., 1992). Poisson's ratio must lie between  $-1$  and  $+0.5$ . These restrictions in turn limit the ratio of the S wave speed to the P wave speed:

$$0 \leq \frac{V_s}{V_p} < \frac{\sqrt{3}}{2} \approx 0.866 .$$

These inequalities define the regions of a hyper-plane in model space, in which real-world materials can lie. In determining values of the objective function, the  $V_s/V_p$  ratios were varied between the above limits, and the density ratio was allowed to vary between 0.5 and 1.5.

## 3. Geometry of the Objective Function

A measure of the ambiguity of the solution to the nonlinear inversion of these P wave reflection amplitudes for the material parameters can be obtained by calculating hyper-planes passing through the point in model space that represents the parameters used to calculate the original synthetic data. We show two key hyper-planes for the top-sand and base-sand reflectors in Figure 2. The density and P wave speed ratios appear to be relatively well resolved against one another (Figure 2a, 2c); the parameters used to calculate the synthetic amplitudes are  $R_p = -0.167$ ,  $\rho_2/\rho_1 = 0.8$  for the top-sand reflector and  $R_p = +0.167$ ,  $\rho_2/\rho_1 = 1.25$  for the base-sand reflector.

In contrast, the  $V_s/V_p$  ratios are poorly resolved against one another. The  $V_s/V_p$  ratios of the shale and gas sand layers are 0.408 and 0.667 respectively. In the case of the base-sand reflector, a single, but elongated, minimum of the objective function is apparent. For the top sand reflector, multiple minima exist in the objective function along a trajectory that extends across much of the range of physically realisable values; non-physical parameter combinations, i.e. negative S wave speed in the lower layer satisfy the amplitude data, but are excluded from Figure 2b by the bounds imposed on the parameters used to calculate the objective function, as discussed previously.

#### 4. Elastic Parameters Derived from P-P Amplitudes

In order to characterise the range of elastic parameters that fit the synthetic amplitude data, we have fixed the value of  $R_p$  to be the actual normal-incidence reflection coefficient, and then calculated values of the objective function. As described previously, we have arbitrarily chosen a RMS misfit of less than 0.01, i.e. values of the objective function less than  $-2$ , to be the set of parameter values that reproduce well the synthetic amplitude data. We have then plotted this volume in the three-dimensional space defined by the density ratio and the two  $V_s/V_p$  ratios. The set of points in model space that are able to reproduce the P wave AVO of the base-sand interface lies parallel to the plane defined by the two  $V_s/V_p$  ratios, and forms a tube restricted to a very narrow range of density values. Thus the density contrast across the base-sand reflector can be well resolved by nonlinear inversion using the exact Zoeppritz equation for the P wave reflection amplitude. The  $V_s/V_p$  ratios are, however, poorly resolved, and a broad range of values is possible. In the case of the top-sand reflector, the volume of points that reproduce the synthetic amplitudes, which approximates a sheet-like structure, extends across almost the entire model space used to calculate values of the objective function. Part of the volume of admissible points occurs at values where the  $V_s/V_p$  ratio in the lower, i.e. gas sand, layer are greater than 0.75, indicating a material with negative Poisson's ratio. Clearly for the top-sand interface, the density and the two  $V_s/V_p$  ratios are all poorly resolved. We ascribe these significant differences between the two interfaces in the regions of model space that satisfy the synthetic amplitude data to the existence of a P wave critical point, which allows the density contrast to be determined, in the case of the base-sand reflector. At a decrease in P wave speed, there is no critical point and the density cannot be resolved.

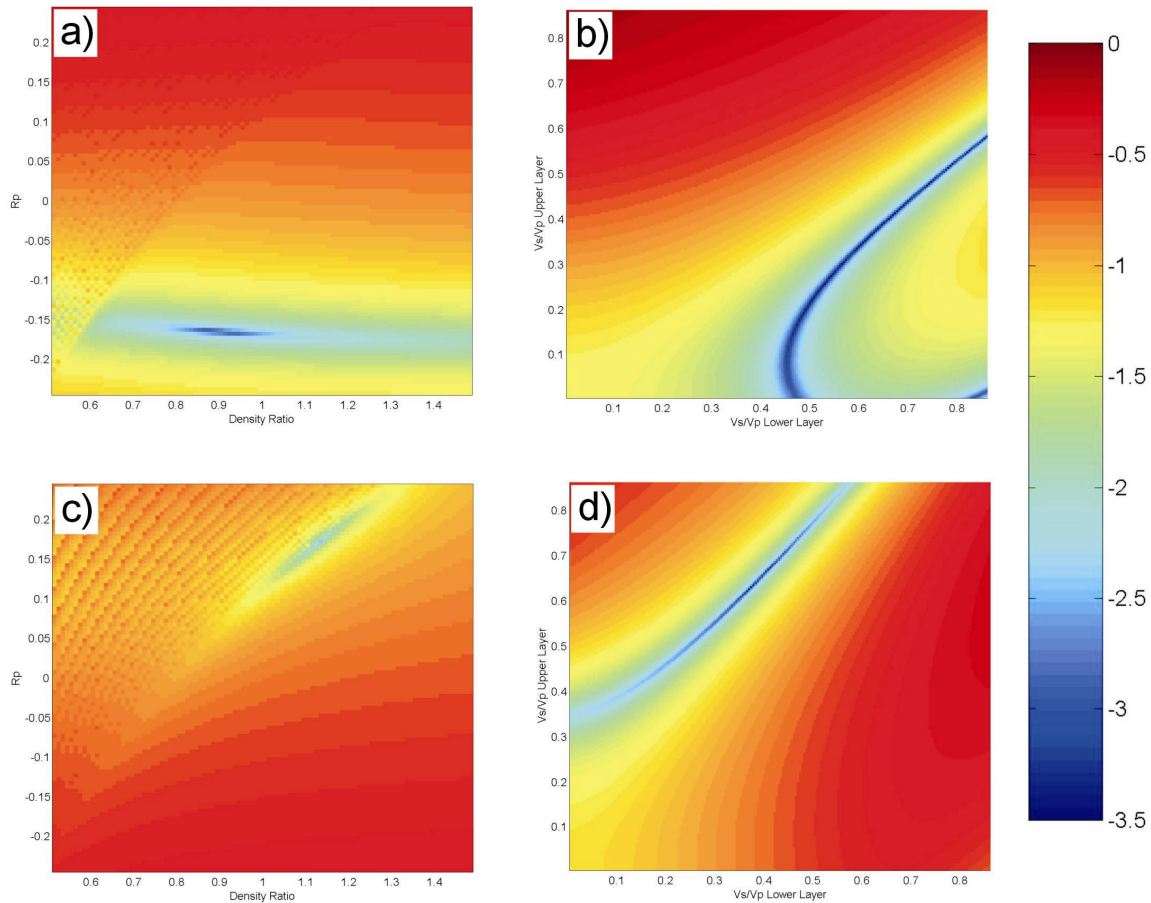


Figure 2. Values of the objective function, i.e.  $\log_{10}$  of the RMS amplitude error, along two hyper-planes through the point in model space that represents the parameters used to calculate the synthetic amplitude data. a)  $R_p - \rho_2/\rho_1$  for top sand, b)  $V_s/V_p$  upper layer –  $V_s/V_p$  lower layer for top sand, c)  $R_p - \rho_2/\rho_1$  for base-sand, d)  $V_s/V_p$  upper layer –  $V_s/V_p$  lower layer for base-sand.

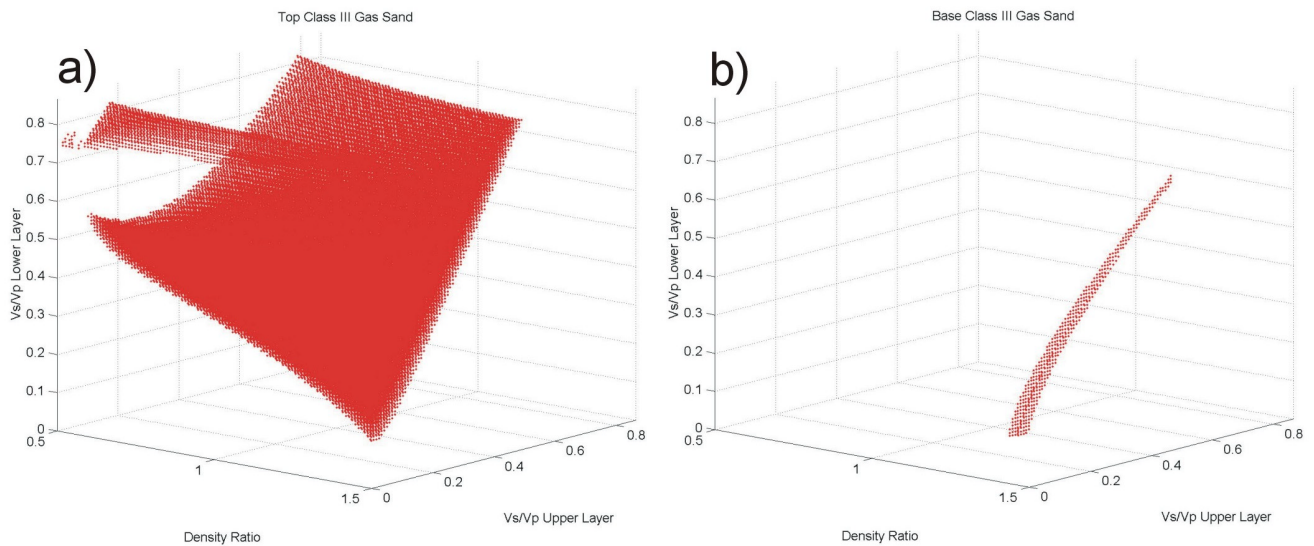


Figure 3. Representation of the regions of model space that can reproduce well the P-P amplitude data, for a correctly specified  $R_p$ . a) Top-sand reflector, b) Base-sand reflector.

### 5. Elastic Parameters Derived from P-P and P-S Amplitudes

To reduce the size of the set of parameter values that will reproduce the synthetic data, and within which a nonlinear inversion scheme must identify a solution, we have modified the objective function to include both P-P and converted P-S reflections. Repeating the preceding analysis, produces the displays shown in Figure 4. For the base-sand interface, Figure 4b indicates that the tradeoff between the two  $V_s/V_p$  ratios is eliminated, and that a global minimum can be isolated by an AVO inversion. The ambiguity in solutions for the top-sand interface is greatly reduced by inclusion of P-S reflections, but a broad range of material properties is still possible, and other a priori constraints are required to identify a meaningful solution.

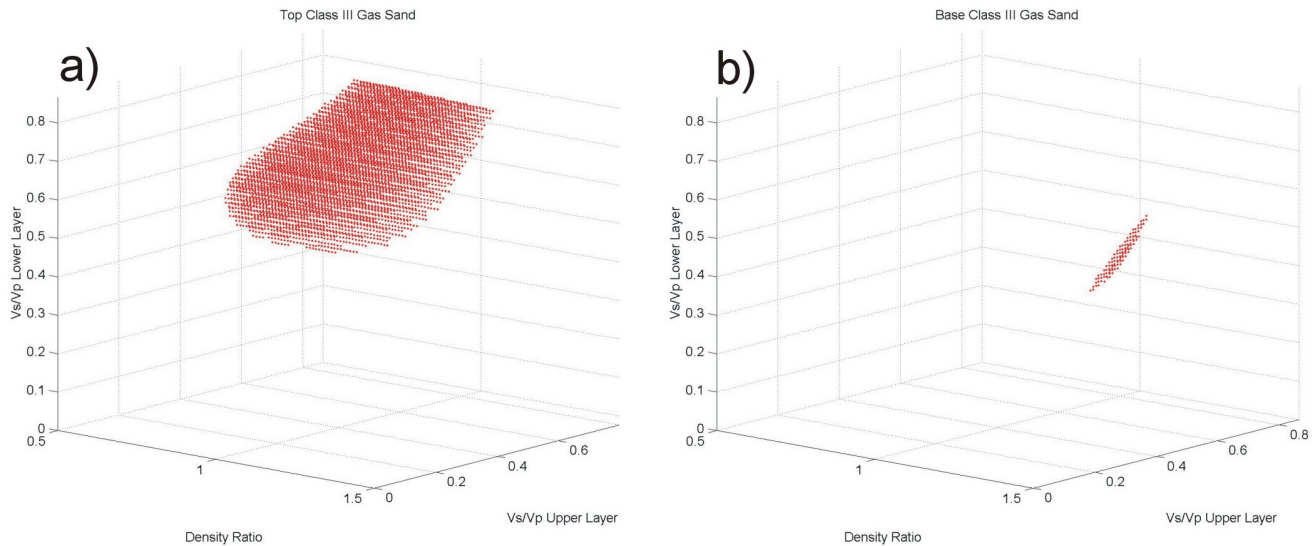


Figure 4. Representation of the regions of model space that can reproduce well both the P-P and P-S amplitude data, for a correctly specified  $R_p$ . a) Top-sand reflector, b) Base-sand reflector.

## Acknowledgements

Jon Downton provided helpful insights insight into linearised inversion methods. This project was funded through the Natural Sciences and Engineering Council of Canada with support from Paradigm Geophysical and Landmark Graphics.

## References

- Aki, K., and Richards, P.G., 1980, Quantitative seismology: W.H. Freeman and Co.
- Debski, W., and Tarantola, A., 1995, Information on elastic parameters obtained from the amplitudes of reflected waves: *Geophysics*, **60**, 1426-1436.
- Fatti, J.L., Smith, G.C., Vail, P.J., Strauss, P.J., and Levitt, P.R., 1994, Detection of gas in sandstone reservoirs using AVO analysis: A 3-D seismic case history using the Geostack technique: *Geophysics*, **59**, 1362-1376.
- Koefoed, O., 1962, Reflection and transmission coefficients for plane longitudinal incident waves: *Geophys. Prosp.*, **10**, 304-351.
- Lines, L., 1999, Density and AVO, *Can. J. Expl. Geophys.*, **35**, 32-35.
- Ostrander, W.J., 1984, Plane-wave reflection coefficients for gas sands at nonnormal angles of incidence: *Geophysics*, **49**, 1637-1648.
- Roberts, G., 2000, Wide-angle AVO, 70th Ann. Internat. Mtg. Soc. Expl. Geophys., Expanded Abstracts, abstract AVO 2.2.
- Shuey, R.T., 1985, A simplification of the Zoeppritz equations: *Geophysics*, **51**, 1983-1903.
- Smith, G.C., and Gidlow, P.M., 1987, Weighted stacking for rock property estimation and detection of gas: *Geophys. Prosp.*, **35**, 993-1014.
- Yeganeh-Haeri, A., Weidner, D.J., and Parise, J.B., 1992, Elasticity of  $\alpha$ -cristobalite: A silicon dioxide with negative Poisson's ratio: *Science*, **257**, 650-652.